HHS Public Access

Author manuscript

*J Nucl Med*. Author manuscript; available in PMC 2019 May 29.

Published in final edited form as:

*J Nucl Med*. 2004 August ; 45(8): 1381–1389.

# PET Imaging of Oncogene Overexpression Using $^{64}$Cu-Vasoactive Intestinal Peptide (VIP) Analog: Comparison with $^{99m}$Tc-VIP Analog

**Mathew L. Thakur, PhD**[1,2], **Mohan R. Aruva, PhD**[1,2], **Jean Gariepy, MD**[3], **Paul Acton, PhD**[4], **Satish Rattan, MD**[5], **Shyam Prasad, PhD**[1,2], **Eric Wickstrom, PhD**[2,6], and **Abass Alavi, MD**[4]

[1]Department of Radiology, Thomas Jefferson University, Philadelphia, Pennsylvania

[2]Kimmel Cancer Center, Thomas Jefferson University, Philadelphia, Pennsylvania

[3]Department of Medical Biophysics, University of Toronto, Toronto, Ontario, Canada

[4]Department of Radiology, University of Pennsylvania, Philadelphia, Pennsylvania

[5]Department of Medicine, Thomas Jefferson University, Philadelphia, Pennsylvania

[6]Department of Biochemistry and Molecular Pharmacology, Thomas Jefferson University, Philadelphia, Pennsylvania

## Abstract

The purpose of this study was to assess the feasibility of PET imaging of oncogene VPAC1 receptors overexpressed in human breast cancer cells.

**Methods:** Vasoactive intestinal peptide (VIP) analog (TP3982) was synthesized to harbor a carboxy-terminus lysine (Lys) residue separated from VIP-asparagine ($Asn^{28}$) by 4-aminobutyric acid (Aba) as a spacer. Lys was derivatized with diaminopropionic acid coupled to a pair of dibenzoylthioglycolic acid residues as protecting groups. The analog was labeled with $^{64}$Cu at pH 9 ($^{64}$Cu-TP3982) and $^{99m}$Tc at pH 12 ($^{99m}$Tc-TP3982). $^{99m}$Tc-TP3982 and VIP derivatized with Aba-GAGG and labeled with $^{99m}$Tc ($^{99m}$Tc-TP3654) were used as reference agents. Smooth muscle relaxivity assays performed with each derivative and compared with unaltered $VIP_{28}$ demonstrated functional integrity. In vitro stability of $^{64}$Cu-TP3982 was determined by challenging the complex with 100-mol excess of diethylenetriaminepentaacetic acid (DTPA), human serum albumin (HSA), and cysteine. In vivo stability was determined in urine and serum for up to 24 h. The mass of the Cu-TP3982 complex was determined by mass spectrometry. Human T47D breast tumor xenografts were grown in athymic nude mice. Planar scintigraphic imaging was performed at 4 and 24 h after the intravenous administration of $^{99m}$Tc-TP3982 and $^{99m}$Tc-TP3654 and PET imaging was performed using a small animal MOSAIC PET scanner, also at 4 and 24 h after injection of $^{64}$Cu-TP3982. Tissue-distribution studies were also performed. In a



For correspondence or reprints contact: Mathew L. Thakur, PhD, Thomas Jefferson University, 1020 Locust St., Suite 359JAH, Philadelphia, PA 19107. Mathew.Thakur@jefferson.edu.

separate experiment, receptors were blocked by intravenous injection of authentic $VIP_{28}$ 30 min before the administration of $^{64}$Cu-TP3982 and tissue distribution was examined.

**Results:** $^{64}$Cu-TP3982 labeling yields were 98% ± 1.2% and those for $^{99m}$Tc-TP3982 and $^{99m}$Tc-TP3654 were 98.2% ± 1.1% and 97% ± 1.6%, respectively. The biologic activity of both VIP analogs was uncompromised. When $^{64}$Cu-TP3982 was challenged with 100-mol excess of DTPA, HSA, or cysteine, >98% radioactivity remained as $^{64}$Cu-TP3982. In vivo, >98% of $^{64}$Cu circulating in plasma remained as $^{64}$Cu-TP3982. Of the $^{64}$Cu excreted in urine 4, 20, and 24 h after injection, >98%, 89.9% ± 0.9%, and 85% ± 3%, respectively, were bound to TP3982. The mass of Cu-TP3982 as determined by surface-enhanced laser desorption/ionization time of flight (SELDI-TOF) was 4,049.7 Da. Four hours after receptor blocking with $VIP_{28}$, there was a significant reduction in uptake of all tissues except in the liver. With $^{64}$Cu-TP3982, the 4-h postinjection tumor uptake was 10.8 ± 2.1 %ID/g versus 0.5 ± 0.02 %ID/g and 0.24 ± 0.08 %ID/g for $^{99m}$Tc-TP3982 and $^{99m}$Tc-TP3654, respectively. Twenty-four hours after injection, the corresponding numbers were 17 ± 0.7 %ID/g, 0.77 ± 0.1 %ID/g, and 0.23 ± 0.1 %ID/g. The severalfold greater uptake (21.2–74) of $^{64}$Cu-TP3982 is attributable to the in vivo stability of the agent.

**Conclusion:** The results suggest that the uncompromised biologic activity and the significantly greater tumor uptake of $^{64}$Cu-TP3982, combined with the high sensitivity and enhanced resolution of PET imaging, make $^{64}$Cu-TP3982 highly desirable for further studies in PET imaging of oncogene receptors overexpressed in breast and other types of cancers.

## Keywords

$^{64}$Cu-VIP analog; imaging oncogene overexpression; PET imaging of oncogene; $^{64}$Cu-VIP breast cancer imaging

---

Functional genomic targeting is a powerful approach not only in oncologic imaging but also in understanding the molecular basis of cancer. Cancer genes are regulated epigenetically, and many tumor types are characterized by their specific gene-expression fingerprints. Named after vasoactive intestinal peptide (VIP) and pituitary adenylate cyclase activated peptide (PACAP), VPAC1 and VPAC2 gene receptors are overexpressed on a variety of tumors (1–3). VIP and PACAP are endogenous growth hormones and have a high affinity for VPAC1 and VPAC2 receptors (4–5).

VIP is a 28-amino acid peptide initially isolated from porcine intestine (6). VIP, whose structure is common in humans, pigs, and rats, is a hydrophobic, basic peptide containing 3 lysine (Lys) (at positions 15, 20, and 21) and 2 arginine (Arg) (at positions 12 and 14) residues. Having an essential histidine (His) residue at the N terminus and an amidated C terminus, all 28 amino acids of VIP are required for full biologic activity (4,5,7). The gene receptors VPAC1 and VPAC2 have been detected on the cell membrane of normal intestinal (8,9) and bronchial epithelial cells (9,10) and are overexpressed on various tumor cells, including colonic adenocarcinomas (9–13), pancreatic carcinoma (14), and carcinoids (8). Because of the hypothesis that VIP labeled with a suitable radionuclide can serve as a tool for molecular imaging and noninvasive, early scintigraphic detection of malignant lesions, VIP has been labeled with $^{123}$I (15), $^{99m}$Tc (16), and $^{64}$Cu (17,18). The $^{123}$I radiolabeling

was facilitated by the 2 tyrosine moieties at positions 10 and 22 in the amino acid sequence of VIP. VIP ($Arg^{15}$,$Arg^{21}$) was also labeled with $^{18}F$ (19). However, molecular modifications were warranted to label VIP with $^{99m}Tc$ or $^{64}Cu$ (16–18). It has been known that His (1) plays a major role in the biologic activity of VIP (7). To facilitate the chelation with these radionuclides, therefore, VIP analogs were prepared by modifying the C terminus at asparagine (Asn) (28).

Although $^{64}Cu$-1,4,8,11-tetraazacyclotetradecane-1,4,8,11-tetraacetic acid (TETA)-VIP was the first $^{64}Cu$-VIP analog to date, no preclinical or clinical data have been reported by these other investigators (17). In contrast, $^{99m}Tc$-VIP, prepared by using Gly-Ala-Gly-Gly($N_4$) as a chelating moiety and 4-ami-nobutyric acid (Aba) as a spacer, has been successfully evaluated for imaging a variety of tumors in humans (20,21).

The high sensitivity and high spatial resolution have rendered PET as one of the leading tools in oncologic imaging. On the basis of the hypothesis that the high sensitivity and high spatial resolution of PET imaging will facilitate detection of small malignant lesions at an early stage, in this study, we prepared and evaluated $^{64}Cu$-VIP analog in vitro and in athymic nude mice bearing human breast tumor xenografts. $^{64}Cu$ chelation was accomplished by synthesizing a protected diaminedithiol ($N_2S_2$)-VIP. Results were compared with $^{99m}Tc$-$N_2S_2$-VIP as well as with $^{99m}Tc$($N_4$)-VIP, which has already been tested in tumorbearing experimental animals (16) and in patients who have different types of cancers (20,21). This article evaluates the potential of the $^{64}Cu$-VIP analog for PET imaging of oncogene overexpression.

## MATERIALS AND METHODS

### Chemicals and Reagents

Benzoyl chloride and stannous chloride were purchased from Sigma-Aldrich Fine Chemicals, Di-Fmoc-diaminopropionic acid from Chem-Impex International, Fmoc-Arg from Peptides International, Inc., Fmoc-amino acids from Calbiochem-Novabiochem Corporation, and the solvents used in peptide synthesis from Caledon. All other chemicals and reagents, including tissue culture media, were obtained from Fisher Scientific.

### $^{64}Cu$

$^{64}Cu$ (half-life = 12.7 h, $\beta^+$ = 655 keV [17.4%], $\beta^-$ = 573 keV [30%]) was obtained from Mallinckrodt Institute of Radiology, Washington University School of Medicine (St. Louis, MO). $^{64}Cu$ is produced in a 12-MeV proton cyclotron using a $^{64}Ni$ (p, n)$^{64}Cu$ nuclear reaction, separated by the method of McCarthy et al. (22,23) and supplied in high specific activity as $CuCl_2$ in 0.1 mol/L HCl. Because of its suitable physical characteristics and ability to form metal chelates, $^{64}Cu$ has been used extensively in the development of several new radiopharmaceuticals, including the $^{64}Cu$-$N_2S_2$ complex such as $^{64}Cu$-ATSM (24–29). $^{99m}Tc$ was obtained as Tc-99m$O_4^-$ from the Thomas Jefferson University Hospital nuclear medicine pharmacy (Philadelphia, PA).

### Synthesis of VIP-Aba-Gly-D-Ala-Gly-Gly

VIP analog conjugated to a chelating moiety was synthesized as described previously (16). A chelating moiety, Gly-(D)Ala-Gly-Gly, provided $N_4$ configuration for metal chelation, and a spacer, γ-Aba, minimized steric hindrance (16). To summarize, the peptide was custom synthesized by PeptidoGenic Research on an ABI 430 synthesizer using a Wang resin. The peptide was cleaved from the resin with 90% trifluoroacetic acid (TFA) and precipitated by the addition of diethylether at −20°C. The product was purified using preparative high-performance liquid chromatography (HPLC; Shimadzu LC-10 AD) and a 5-μm $C_{18}$ HAIsil column. Fractions were collected and lyophilized, and the resultant compounds were characterized using a Perkin Sciex APZ ion-spray mass spectrometer. VIP-Aba-Gly-Gly-D-Ala-Gly had the observed molecular weight of 3,654.48, which is very similar to the theoretically expected molecular weight of 3,654.43. This analog is referred to as TP3654.

### Synthesis of $N_2S(benzyl)_2$-containing VIP

A VIP harboring a C-terminal diaminodithiol ($N_2S_2$) chelator was synthesized (30) on a Wang resin using an ABI 341A peptide synthesizer (Applied Biosystems Inc.). Briefly, FmocLys (ivDde) was first introduced at the C terminus of the peptide, followed by γ-Aba. The 28-amino acid–long VIP sequence was then assembled by standard Fmoc chemistry with the final histidyl residue being a *t*-butoxycarbonyl (*t*-BOC)–protected His(Trt) derivative. The capping *t*-BOC function was necessary to ensure that the N-terminus amino group remained protected during subsequent deprotection and coupling cycles performed at the ε-amino group of the C-terminal Lys. The ivDde group at the C-terminal Lys was then selectively removed with 2% hydrazine, followed by the successive additions of di-Fmoc-L-diaminopropionic acid, and S-benzoylthioglycolic acid. The resulting protected diaminedithiol ($N_2$S-benzoyl)$_2$–containing VIP was cleaved from the resin using TFA-to-water-to-phenol-to-thioanisole-to-ethanedithiol (EDT) (82.5:5:5:5:2.5) mixture and precipitated with diethyl ether. The crude peptide was purified to homogeneity by reverse-phase HPLC (Waters, Millipore) on a Vydec C4 column (5 μm, 10 mm × 250 mm). The mass of the VIP-chelator construct was confirmed by electrospray mass spectrometry: *m/z* observed, 3,982.67 ($M+H^+$); calculated, 3,982.53. The analog was named TP3982 and is presented in Figure 1.

### Functional Assay Using Opossum (*Dedelphis virginiana*) Internal Anal Sphincter (IAS) Smooth Muscle Tissues

To examine the biologic activity of the 2 analogs, the IAS smooth muscle assays were performed, in which $VIP_{28}$ was used as a control. The assay is based on the binding of VIP to specific receptors that causes a concentration-dependent decrease in the resting tension of the IAS smooth muscle. The effects of different concentrations of VIP and its analogs were determined until maximum fall in the basal tension of IAS was reached.

### Preparation of Smooth Muscle Strips

Adult opossums of either sex were anesthetized with sodium pentobarbital (40 mg/kg intraperitoneally) and then were killed. The anal canal was removed and was transferred quickly to oxygenated Krebs' physiologic solution of the following composition (in

mmol/L): 118.07 NaCl, 4.69 KCl, 2.52 $CaCl_2$, 1.16 $MgSO_4$, 1.01 $NaH_2PO_4$, 25 $NaHCO_3$, and 11.10 glucose. The adhering blood vessels and extraneous tissues that contained the external anal sphincter were removed by sharp dissection, and the anal canal was opened and pinned flat with the mucosal side up on a dissecting tray containing oxygenated Krebs' solution. The mucosa was removed by using forceps and fine scissors, and IAS circular smooth muscle strips (approximately 2-mm wide and 1-cm long) were cut from the lowermost part of the anal canal. Silk sutures were tied to both ends of these muscle strips for isometric tension measurements.

## Measurement of Isometric Tension

The IAS smooth muscle strips were transferred to temperature-controlled 2-mL muscle baths containing Krebs' solution bubbled continuously with a mixture of 95% $O_2$ and 5% $CO_2$.

One end of the muscle strip was tied to the bottom of the muscle bath with the tissue holder, and the other end was attached to an isometric force transducer (model FTO3; Grass Instruments Co.). Isometric tensions of the smooth muscle strips were recorded on a Beckman Dynograph recorder (Beckman Instruments). Initially, 1 g of tension was applied to the muscle strips, which were then allowed to equilibrate for about 1 h with occasional washings. During this equilibration period, strips developed steady tension. Only strips that developed steady tension and relaxed in response to electrical field stimulation were used. Both optimal length and base line of the muscle strips were determined, as described previously (7,16–18).

## Drug Responses

The effect of different concentrations of these analogs on resting IAS tension was examined using cumulative concentration responses. After a given concentration–response curve was derived, the muscle strips were washed continuously for 45–60 min before testing for the concentration–response curve of another agent. Maximal relaxation (100%) of the smooth muscle strips was determined after completely relaxing the muscle strips with 5 mmol/L ethylenediaminetetraacetic acid (EDTA).

## Preparation and Quality Control of $^{99m}$Tc-TP3654

We added 10 μg TP3654 in 0.05 mol/L acetate buffer (pH 4.6); 50 μg $SnCl_2 \cdot H_2O$ in 10 μL, 0.05 mol/L HCl; and 300 μL, 0.1 mol/L trisodium phosphate (pH 12.0) to a clean, nitrogen-flushed, 10-mL glass vial. The content was frozen immediately by placing the vial in an acetone dry ice bath. The vial was then placed in a GeneVac lyophilizer and was lyophilized for 2 h. The vials were then filled with nitrogen, sealed, and stored at −20°C.

We added 370–1,480 MBq (10–40 mCi) $^{99m}$Tc in 0.1–0.6 mL, 0.9% NaCl to a TP3654 vial at 22°C and mixed using a vortex mixer. The mixture was incubated for 15 min. Then the pH of the reaction mixture was raised to 6.0–6.5 by the addition of 1.0–1.5 mL of 0.1 mol/L $NaH_2PO_4$ solution, which had a pH of 5.2. Ascorbic acid (500 μg) was then added as a stabilizing agent. HPLC analysis was performed using a Rainin HPLC with a reverse-phase $C_{18}$ microbond column and with 0.1% TFA in $H_2O$ (solvent A) and 0.1% TFA in acetonitrile

(solvent B). The gradient was such that solvent B was 10% at 0 min and 90% at 28 min. In instant thin-layer chromatography (ITLC-SG; Gelman Sciences) using a pyridine-acetic acid-water (3:5:1.5) mixture as a mobile phase, colloid remains at $R_f$ 0.0 and $^{99m}$Tc-TP3654 migrates at $R_f$ 1.0. When methyl ethylketone (MEK) is used as mobile phase, $^{99m}$Tc-TP3654 remains at $R_f$ 0.01 and free $^{99m}$Tc migrates at $R_f$ 1.0.

### Preparation of $^{99m}$Tc-TP3982 and Quality Control

We dispensed 10 μg TP3982 in a 5-mL glass test tube to which were also added 40 μg $SnCl_2$ in 4-μL, 0.05-mol/L HCl, 370–740 MBq (10–20 mCi) $^{99m}$Tc in 200-μL, 0.09% NaCl, and 300 μL of 0.05 mol/L $Na_3PO_4$, at a pH of 12. The reaction mixture was vortexed and incubated at room temperature for 30 min. We added 1 mL of 0.05 mol/L $NaH_2PO_4$ solution (pH, 4.5) to neutralize the pH and performed quality control using HPLC as described previously. ITLC analysis was also performed, using the same procedure applied for the quality control of $^{99m}$Tc-TP3654.

### Preparation of $^{64}$Cu-TP3982 and Quality Control

We dispensed 20 μg of TP3982 in 200 μL of 0.2 mol/L glycine buffer (pH, 9) in a 5-mL glass test tube. A required quantity (11.1–15.8 MBq [300–500 μCi]) of $^{64}$Cu in 2-μL, 0.1-mol/L HCl was then added. This was followed by the addition of 60 μg of $SnCl_2$ in 3-μL, 0.1-mol/L HCl as a deprotecting agent. The mixture was vortexed and incubated at 90°C for 20 min. HPLC and ITLC analyses were performed as described for the analyses of $^{99m}$Tc-TP3654 and $^{99m}$Tc-TP3982.

### Stability of TP3654 and TP3982

When TP3982 is labeled with $^{99m}$Tc at pH 12 and with $^{64}$Cu at pH 9, a 20-min incubation at 90°C is required. The stability of the peptide after the above treatment at the respective high-pH solutions was examined by HPLC and ultraviolet (UV) absorbance at 280 nm. TP3982, not treated as above, served as a control. TP3654 was also treated and analyzed similarly.

### Stability of $^{64}$Cu-TP3982 Ex Vivo and In Vivo

To examine the thermodynamic stability, $^{64}$Cu-TP3982 was incubated at 37°C for 2 h with 100-mol excess of diethylenetriaminepentaacetic acid (DTPA), human serum albumin (HSA), and cysteine. Solutions were then analyzed by ITLC using MEK and ethyl acetate as mobile phases. In either case, $^{64}$Cu-TP3982 remains at $R_f$ 0.0 and free $^{64}$Cu migrates at $R_f$ 1.0.

To examine in vivo stability, 3.7 MBq (100 μCi) of $^{64}$Cu-TP3982 were injected intravenously to nude mice, and urine samples were collected 2, 4, 20, and 24 h after injection, and plasma was collected 4 and 24 h after injection. Analyses were performed using ITLC, with MEK and ethyl acetate as mobile phases. The small amount of $^{64}$Cu recovered both in urine and plasma samples prevented analysis of the samples by radio-HPLC.

## Mass Spectroscopic Analysis

We allowed 5 μmol copper as cupric chloride to react with 1 μmol TP3982 in glycine buffer with pH 9, and the reaction mixture was analyzed by HPLC, as described previously. A 2-mL fraction was collected to encompass the Cu-TP3982 mass at retention time ($R_t$) 8 min. The solvent was evaporated in speedvac, and the complex was analyzed using surface-enhanced laser desorption/ionization time of flight (SELDI-TOF-MS; Ciphergen Corp.).

## Animal Imaging and Tissue-Distribution Studies

Estrogen-dependent human T47D breast tumor cells (American Type Culture Collection) are known to express VPAC1 receptors (31). For cell preparation and implantation, cells were grown in exponential growth (~$2 \times 10^7$ per T-75 flask) in Dulbecco's modification of Eagle medium (DMEM) containing heat-inactivated 10% fetal bovine serum at 37°C in 5% $CO_2$/95% air. Cells were harvested using 0.25% trypsin-EDTA solution, washed with DMEM, and resuspended to a concentration of approximately $20 \times 10^6$ cells per milliliter. Cell count was determined using a hemocytometer and a light microscope, and cell viability was assessed using trypan blue-dye exclusion.

Approximately $4 \times 10^6$ viable cells in 20 μL were then implanted subcutaneously in the right thigh of each athymic BALB/c female nude mouse weighing 20–25 g. Tumors were allowed to grow to no more than 1 cm in diameter. All animal experiments were performed using a protocol approved by the Association for Assessment and Accreditation of Laboratory Animal Care-certified institutional animal care and use committee.

## Imaging

Animals given $^{99m}$Tc-TP3982 or $^{99m}$Tc-TP3654 were used as a control and imaged using a General Electric STARCAM $\gamma$-camera equipped with a low-energy, parallel-hole collimator and a dedicated computer. Mice were imaged at arbitrarily chosen time periods of 4 or 24 h after injection. Animals were either killed with halothane inhalation immediately before imaging or anesthetized with isoflorane during imaging.

Mice that were to be killed at 4 h after injection received 7.4 MBq (200 μCi) of the $^{99m}$Tc agent and those that were to be killed 24 h after injection received 25.9 MBq (700 μCi). The volume of each injection was 200 μL given intravenously through a lateral tail vein. Radioactivity in the syringe was measured in a Capintec CR 15 R dose calibrator before and after administration, so that the exact quantity received by each animal could be determined.

PET imaging was performed using a Philips MOSAIC small animal scanner at the University of Pennsylvania (32). This device uses a discrete $2 \times 2 \times 10^3$ mm gadolinium-oxyorthosilicate (GSO), Anger-logic detector for use in high-resolution (2 mm), high-density, and high-counting-rate animal PET imaging. It has a 21-cm diameter and 12.8-cm transverse field of view and operates exclusively in 3-dimensional (3D) volume imaging mode. During imaging, animals were lightly anesthetized with 1.5% isoflurane in 1 L/min oxygen. Approximately 3.33 MBq (90 μCi) of $^{64}$Cu-TP3982 were injected through a lateral tail vein, and animals were imaged 4 and 24 h after injection. Up to 27 million counts were

collected. Images were reconstructed using fully 3D iterative reconstruction algorithm, giving a pixel size of 1 mm (33). Region-of-interest (ROI) analysis was performed digitally.

### Tissue-Distribution Studies

Four or 24 h after injection ($n = 5$) animals were killed by halothane inhalation; tissues were dissected, washed free of blood, blotted dry, and weighed in an analytic balance; and associated radioactivity was counted in an appropriate energy window (±20%) in a Packard 5000 series $\gamma$-counter. Results were calculated as percentage injected dose per gram (%ID/g) of tissue and analyzed using the Student $t$ test.

### Receptor Blocking

To determine whether $^{64}$Cu-TP3982 uptake was receptor specific, we blocked the VPAC1 receptors by intravenous administration of 50 μg of $VIP_{28}$, 30 min before the administration of $^{64}$Cu-TP3982. The study was performed in a separate group ($n = 5$) of mice bearing T47D tumors, and the protocol described in the Tissue Distribution section was followed.

## RESULTS

The schematic diagram for the preparation of TP3982 is given in Figure 1. The molecular weight of TP3982, as determined by mass spectrometry, was 3,982.82 compared with the theoretic molecular weight of 3,982.53. The purity was >98%. TP3654 synthesis was performed as described previously (16). The observed molecular weight was 3,654.32 compared with the theoretic weight of 3,654.48, and purity was >98%. The data with functional activity of different VIP analog are given in Figure 2. The data depict that at $1 \times 10^{-6}$ mol/L of TP3982, 92.1% ± 2.9% of muscle relaxivity was achieved. This was slightly greater than that of native VIP but similar to that of TP3654, which has been used successfully in humans. These data suggest that the biologic activity of TP3982 was not compromised.

### Stability of TP3654 and TP3982

The HPLC $R_t$ values for TP3654 and TP3982, as determined by UV absorbance at 280 nm, were 12 min and 15 min, respectively. After reacting the peptides at their respective radiolabeling buffers at high pH and heat, the peptides were eluted at the same $R_t$ values and no detectable fragments were seen in the HPLC elutions, thereby indicating the stability of the peptides.

### Stability of $^{64}$Cu-TP3982 Ex Vivo and In Vivo

As determined by ITLC, >98% of $^{64}$Cu remained bound to TP3982 after incubation with 100-mol excess of DTPA, HSA, or cysteine. In plasma, >98% of $^{64}$Cu was bound to TP3982 at both time points. In urine, >98% $^{64}$Cu was bound to TP3982 for up to 4 h after injection. However, at 20 and 24 h after injection, 85% ± 3% and 89.9% ± 0.9%, respectively, of the radioactivity excreted in urine was associated with TP3982.

## Mass Spectrometric Analysis

The SELDI-TOF-mass spectrum given in Figure 3 shows that the mass of Cu-TP3982 complex was 4,049.7 Da compared with the calculated mass of 4,047 Da. The unreacted TP3982 was also detectable at mass 3,982.7 Da.

## Tissue Distribution

The $^{64}$Cu-TP3982 preparations (specific activity = 2.22–11.1 GBq/μmol [60–300 mCi/μmol]) had a single radio-HPLC peak at $R_t$ 8.2 min (Fig. 4), 98% ± 1.2% labeling efficiency, and 1.2% ± 0.5% colloid formation. Tissue distribution of $^{99m}$Tc-TP3654 and $^{99m}$Tc-TP3982 is given in Table 1. Data indicate that, in general, the tissue uptake of $^{99m}$Tc-TP3982 was significantly greater than that of $^{99m}$Tc-TP3654 in all tissues, except in the kidneys at 4 h after injection. Kidney uptake of $^{99m}$Tc-TP3982 was lower than that of $^{99m}$Tc-TP3654 at 4 h but was greater at 24 h, thereby indicating a slow elimination of the agent via the kidneys. With $^{99m}$Tc-TP3982, the tumor uptake was significantly greater than $^{99m}$Tc-TP3654 at both time periods, but tumor-to-muscle ratios were lower because of the higher muscle uptake of $^{99m}$Tc-TP3982. The tumor-to-blood ratios were slightly better for $^{99m}$Tc-TP3982 at 24 h but not at 4 h after injection. These data suggest that, for the $^{99m}$Tc tracer, the use of an $N_2S_2$ chelating moiety did not provide enough advantage to warrant its exclusive use.

The tissue distribution of $^{64}$Cu-TP3982 and $^{99m}$Tc-TP3982 is given in Table 2. At both time points, the $^{64}$Cu-TP3982 distribution was significantly greater than that of $^{99m}$Tc-TP3982 for all tissues, including that for the tumor. The data indicate that the blood clearance of $^{64}$Cu-TP3982 was slow, as was the renal clearance. However, the radioactivity in the lungs and liver significantly decreased ($P < 0.05$) as the time after injection increased. In all other tissues the radioactivity increased. The tumor uptake also increased from 10.8 ± 2.1 %ID/g 4 h after injection to 17 ± 0.7 %ID/g 24 h after injection. The tumor uptake of $^{64}$Cu-TP3982 was 21.2 times greater 4 h after injection and 22.1 times greater 24 h after injection than that of $^{99m}$Tc-TP3982. Compared with the tumor uptake of $^{99m}$Tc-TP3654, the tumor uptake of $^{64}$Cu-TP3982 was 45 times greater 4 h after injection and 74 times greater 24 h after injection. The tumor-to-muscle and tumor-to-blood ratios for $^{64}$Cu-TP3982 were 6.4 ± 2.3 and 6 ± 4.3 and 6.4 ± 0.9 and 7 ± 3.4 at 4 and 24 h after injection, respectively. Significantly smaller ratios for control agents are evident in Tables 1 and 2.

## Imaging

In Figure 5, 24-h posterior images of nude mice bearing human breast cancer T47D in the right thigh are shown. The planar $\gamma$-camera image at the left is that of a mouse that received $^{99m}$Tc-TP3654; the middle image is also a planar $\gamma$-camera image of a mouse that received $^{99m}$Tc-TP3982. The image at the right is the 1-mm coronal PET image of a mouse that received $^{64}$Cu-TP3982. The enhanced tumor uptake of $^{64}$Cu-TP3982 is clearly evident. As determined by the digital ROI analysis, radioactivity in the tumor was 9.15 ± 0.5 greater than the contralateral thigh muscle 4 h after injection and 13.9 ± 0.7 greater 24 h after injection.

### Receptor Blocking

The results of receptor-blocking experiments are given in Table 3. Four hours after injection of $^{64}$Cu-TP3982, the distribution of $^{64}$Cu in mice given 50 μg of $VIP_{28}$ 30 min before the injection was significantly decreased in all tissues (including the tumor) except the liver. Twenty-four hours after injection, the tissue radioactivity levels in treated mice were not significantly different from those in unblocked mice, except in the muscle, intestine, heart, and tumor. The lung uptake decreased from 50 ± 8 %ID/g to 5.4 ± 0.3 %ID/g 4 h after injection and from 11 ± 5.1 %ID/g to 7.1 ± 0.7 %ID/g 24 h after injection. The tumor uptake decreased from 10.8 ± 2.3 %ID/g to 6.4 ± 1.1 %ID/g and from 17 ± 0.7 %ID/g to 12.1 ± 0.01 %ID/g, 4 and 24 h after injection, respectively.

## DISCUSSION

The high sensitivity and excellent spatial resolution of PET scanners has revolutionized the field of nuclear medicine and provided a new tool in oncologic, cardiac, and neurologic imaging. PET imaging cannot only localize occult malignant lesions but also can determine the effectiveness of their therapeutic or surgical interventions. $^{64}$Cu is one of the few useful metallic, positron-emitting radionuclides that not only has a half-life (12.7 h) long enough to transport it from one end of a country to the other but also permits studies to be performed for 24 h or longer after it has been administered without excessive decay having occurred. The chemistry of Cu is well known and a variety of Cu chelates, including Cu-$N_2S_2$, have been prepared (23–29,34,36). The role of Cu in biologic systems is also well known (34,35). The $^{64}$Cu radionuclide, therefore, has been evaluated extensively in PET imaging as well as, when injected in large quantities, in therapeutic applications (36).

In recent years, molecular imaging has gained increased attention, and in preclinical studies, a variety of animals models have played a vital role. In such studies, small animal PET equipment has been shown to be very useful because it provides metabolic, functional, and molecular information noninvasively and quantitatively (37).

Over the past few years, we have gained extensive experience in imaging oncogenic overexpression noninvasively, both in experimental animals (16,38,39) and in a limited number of humans (20,21). In human studies $^{99m}$Tc-VIP analogs were used. The VIP analogs detected all tumors correctly that expressed VIP receptors, including the 2 that were not detectable by other routine nuclear medicine techniques. One tumor was a high-grade spindle cell sarcoma in the neck of a 20-y-old patient, and the other tumor was a ductal epithelial hyperplasia atypia in a 42-y-old female. These promising results in detecting occult tumors in humans were possible despite the 0.3 %ID/g (Table 1) uptake of $^{99m}$Tc-TP3654 in all experimental human tumors that were grown in athymic nude mice.

With the hypothesis that the high resolution and better sensitivity of PET scanners will allow researchers to detect small, malignant breast tumors with lower radioactivity dose than normally required for planar or SPECT $\gamma$-camera imaging, we chose to evaluate the use of a $^{64}$Cu-VIP analog in preclinical studies. The VIP analog TP3654 could be labeled with $^{64}$Cu. However, yields were low and variable. VIP was therefore modified to incorporate $N_2S_2$ chelating moiety (TP3982), as described previously. $^{64}$Cu-TETA-VIP was prepared

previously (17), but no further preclinical or clinical studies have been reported. The $^{64}$Cu-TP3982 yields, as reported here, were not only higher than $^{64}$Cu-TP3654 but were also consistently reliable. This prompted us to choose this analog for further investigation.

The IAS muscle relaxation data demonstrated that the biologic activity of TP3982 was well preserved and comparable with $VIP_{28}$ and TP3654. When challenged with 100-mol excess of DTPA, HSA, or cysteine, >98% of $^{64}$Cu remained chelated with TP3982. The stability of $^{64}$Cu-TP3982 was also evident in vivo, because >98% $^{64}$Cu activity circulating in plasma remained bound to TP3982. Similarly, >98% of the radioactivity excreted in urine was bound to TP3982, although 11.1% ± 0.9% and 15% ± 3% of $^{64}$Cu was found not to be associated with TP3982 at 20 and 24 h after administration, respectively. These results compared favorably with those of $^{99m}$Tc-TP3654, the urinary-HPLC analysis of which indicated greater biodegradation (16).

The mass of the Cu-TP3982 complex as determined by SELDI-TOF-mass spectrometry was 4,049 Da compared with the calculated mass of 4,047. The unreacted peptide, with its original mass of 3,982 Da, provided further evidence that the high pH did not degrade the peptide. Approximately 10% of the Cu-TP3982 was chloroform extractable, indicating that the complex was not lipophillic.

VIP, an endogenous 28-amino acid hormone, is known to be susceptible to proteolytic degradation. Our data suggest that the analog TP3982 not only retains the biologic activity of native $VIP_{28}$ but also is resistant to proteolysis. The reasons for this favorable behavior of TP3982 are not understood.

The tumor uptake of $^{64}$Cu-TP3982 was up to 74 times greater than that of $^{99m}$Tc-TP3982 or $^{99m}$Tc-TP3654. These results can be attributed to the in vivo stability of $^{64}$Cu-TP3982. Furthermore, one possible reason for the lower tumor uptake of $^{99m}$Tc-VIP analogs may be that, once taken up by tumors or tissue, the reduced $^{99m}$Tc can be oxidized to $^{99m}Tc^{7+}$ and egressed out, thereby giving low tumor and tissue uptake. As a function of time elapses, such a decrease in tumor and other tissue uptake of $^{99m}$Tc-labeled peptides is not uncommon (40).

The reasons for the slower blood clearance of $^{64}$Cu-TP3982 compared with that of $^{99m}$Tc-TP3654 are not yet clear but may be related to the in vivo stability and resistance to proteolytic metabolism of $^{64}$Cu-TP3982. The increase in most major tissues and in the tumor supports this explanation because $^{64}$Cu-TP3982–circulating molecules may have continued to bind to the specific receptors expressed on the cells of these tissues, albeit at different density. Our blocking data show that the uptake was receptor specific. The improved tumor uptake at early time points and at a long time after injection is rewarding. The tumor uptake and tumor-to-muscle and tumor-to-blood ratios were also sufficiently high to perform imaging 4 h after injection. Studies in which imaging takes place before 4 h after injection have not been performed yet.

We believe that this enhanced, receptor-specific tumor uptake of $^{64}$Cu-TP3982 combined with the high sensitivity and improved resolution of PET scanners will allow us to localize smaller malignant breast lesions or other types of tumors that overexpress VPAC1 or VPAC2

receptors, with high sensitivity and specificity. PET imaging performed while the patient is lying in the prone position will further improve sensitivity because the negligible normal breast tissue uptake may provide high contrast and eliminate any interference from the radioactivity in the lungs, heart, blood pool, liver, or spleen. Dedicated breast PET imaging devices under development will facilitate further such imaging and may contribute to unequivocal delineation of small malignant breast lesions.

For diagnostic imaging, 107.3–129.5 MBq (2.9–3.6 mCi) of $^{64}$Cu-TETA-octreotide has been administered to human subjects without the risk of excessive radiation dose (29). With high tumor uptake, the high sensitivity of PET scanners, and the low background for imaging in the prone position, it may be feasible to inject a smaller dose without compromising image quality.

We conclude that $^{64}$Cu-TP3982 is a novel and promising agent for PET imaging of oncogene overexpression. The entire study was fruitful. Particularly noteworthy were the study's in vivo stability and up to 74-times greater tumor uptake than that of $^{99m}$Tc-TP3654, which we have already used successfully in humans in imaging tumors that express VPAC1 oncogene. We believe that these qualities of $^{64}$Cu-TP3982 support our hypothesis and warrant further investigation. On the basis of these data, it is also reasonable to speculate that equally good results could be achieved with a similar analog of PACAP, which recognizes both VIP and PACAP oncogene receptors overexpressed on many human tumors (1–6).

## ACKNOWLEDGMENTS

The production and supply of $^{64}$Cu was supported by National Institutes of Health (NIH) grant 1R24 CA86307 (principal investigator, Michael Welch, Mallinckrodt Institute of Radiology, Washington University, St. Louis, MO). The skillful assistance of Christopher Cardi in PET imaging and Eleonora Bolewska-Pedyczak in peptide synthesis is gratefully acknowledged. The work was also supported in part by NIH grants HL 59769 and CA 42960, Department of Energy grant ER63055, and the Canadian Breast Cancer Research Alliance. We thank Kate Musselman for the preparation of the manuscript.

## REFERENCES

1. Reubi JC. In vitro identification of vasoactive intestinal peptide receptors in human tumors: implications for tumor imaging. J Nucl Med. 1995;36:1846–1853. [PubMed: 7562054]
2. Reubi JC, Laderach U, Waser B, Gebbers JO, Robberecht P, Laissue JA. Vasoactive intestinal peptide/pituitary adenylate cyclase activating peptide receptor subtypes in human tumors and their tissues of origin. Cancer Res. 2000;60:3105–3112. [PubMed: 10850463]
3. Reubi JC, Waser B, Laderach U, Srinivasan A. Pituitary adenylate cyclase activating polypeptide (PACAP) and PACAP II receptors in human tumors: in vitro binding of DTPA-linked PACAP analogs [abstract]. Eur J Nucl Med. 1997;24:1058.
4. Zia H, Hida T, Jakowlew S, et al. Breast cancer growth is inhibited by VIP hybrid, a synthetic VIP receptor antagonist. Cancer Res. 1996;56:3486–3489. [PubMed: 8758916]
5. Zia H, Leyton J, Loecho T, et al. PACAP receptors are present on breast cancer cell lines. Am Assoc Cancer Res. 1997;38:117.
6. Said SI, Mutt V. Polypeptide with broad biological activity: isolation from the small intestine. Science. 1970;69:1217–1218.
7. Chakder S, Rattan S. The entire vasoactive intestinal polypeptide molecule is required for the activation of the vasoactive intestinal polypeptide receptor: functional and binding studies. J Pharm Exp Ther. 1993;266:392–399.

8. Virgolini I, Yang Q, Li S, et al. Cross-competition between vasoactive intestinal peptide and somatostatin for binding to tumor cell membrane receptors. Cancer Res. 1994;54:690–700. [PubMed: 7905785]
9. Blum AM, Mathew R, Cook GA, Metwali A, Felman R, Weinstock JV. Murine mucosal T cells have VIP receptors functionally distinct from those on intestinal epithelial cells. J Neuroimmunol. 1992;39:101–108. [PubMed: 1320055]
10. Couvineau A, Luburthe M. The human vasoactive intestinal peptide receptor: molecule identification by covalent cross-linking in colonic epithelium. J Clin Endocrinol Metab. 1985;61:50–55. [PubMed: 2987295]
11. Paul S, Said SI. Characterization of receptors for vasoactive intestinal peptide solubilized from the lung. J Biol Chem. 1987;262:158–162. [PubMed: 3025200]
12. Sreedharan SP, Robichon A, Peterson KE, Goetzl EJ. Cloning and expression of the human vasoactive intestinal peptide receptor. Proc Natl Acad Sci USA. 1991;88:4986–4990. [PubMed: 1675791]
13. el Battari A, Martin JM, Luis J, et al. Solubilization of the active vasoactive intestinal peptide receptor from human colonic adenocarcinoma cells. J Biol Chem. 1988;263:17685–17689. [PubMed: 2846575]
14. Svoboda M, De Neef P, Tastenoy M, Christophe J. Molecular characterization and evidence for internalization of vasoactive intestinal peptide (VIP) receptors in the tumoral rat-pancreatic acinar cell line AR 4-2 J. Eur J Biochem. 1988; 176:707–713. [PubMed: 2844535]
15. Virgolini I, Raderer M, Kurtaran M, et al. Vasoactive intestinal peptide receptor imaging for the localization of intestinal adenocarcinomas and endocrine tumors. N Engl J Med. 1994;331:1116–1121. [PubMed: 7935635]
16. Pallela VR, Thakur ML, Chakder S. Tc-99m labeled vasoactive intestinal peptide receptor agonist: functional studies. J Nucl Med. 1999;40:352–360. [PubMed: 10025846]
17. Chen X, Edwards WB, Anderson CJ, McCarthy TJ, Welch MJ. Solid phase synthesis of teta conjugated vasoactive intestinal peptide and in vivo behavior of copper-64 radiolabeled VIP conjugate. J Labelled Compds Radiopharm. 2001; 44:S688–S690.
18. Thakur ML, Aruva M, Bolewska-Pedyczak E, Gariepy J. Preparation of Cu-64 and Tc-99m-N2S2-vasoactive intestinal peptide (VIP) for imaging gene expression [abstract]. J Labelled Compds Radiopharm. 2003;46:S128.
19. Moody TW, Leyton J, Unsworth E, John C, Lang L, Eckelman WC. ($Arg^{15}$, $Arg^{21}$) VIP: a VIP agonist for localizing breast cancer tumors. Peptides. 1998; 19:585–592. [PubMed: 9533649]
20. Thakur ML, Marcus CS, Saeed S, et al. $^{99m}$Tc-Labeled vasoactive intestinal peptide analog for rapid localization of tumors in humans. J Nucl Med. 2000;41: 107–110. [PubMed: 10647612]
21. Thakur ML, Marcus CS, Saeed S, et al. Imaging tumors in humans with Tc-99m-VIP In: Fahrsenkrug J, Said SI, eds. VIP, PACAP, Glucagon, and Related Peptides: Annals of the NY Academy of Science. Vol. 921 New York, NY: New York Academy of Science; 2001:37–43.
22. McCarthy DW, Shefer RE, Klinkowstein RE, et al. Efficient production of high specific activity $^{64}$Cu using a biomedical cyclotron. Nucl Med Biol. 1997;24:35–43. [PubMed: 9080473]
23. Obata A, Kasamatsu S, McCarthy DW, et al. Production of therapeutic quantities of $^{64}$Cu using a 12 MeV cyclotron. Nucl Med Biol. 2003;30:535–539. [PubMed: 12831992]
24. Lewis JS, Laforest R, Buettner TL, et al. Copper-64-diacetyl-bis($N^4$-methylthiosemicarbazone): an agent for radiotherapy. Proc Natl Acad Sci USA. 2001;98: 1206–1211. [PubMed: 11158618]
25. Dearling JLJ, Lewis JS, Mullen GED, Rae MT, Zweit J, Blower PJ. Design of hypoxia-targeting radiopharmaceuticals: selective uptake of copper-64 complexes in hypoxic cells in vivo. Eur J Nucl Med. 1998;25:788–792. [PubMed: 9662602]
26. Lewis JS, McCarthy DM, McCarthy TJ, Fujibayashi Y, Welch MJ. Evaluation of 64-Cu-ATSM in vitro and in vivo in a hypoxic tumor model. J Nucl Med. 1999;40:177–183. [PubMed: 9935074]
27. Anderson CJ, Schwarz SW, Connett JM, et al. Preparation, biodistribution, and dosimetry of copper-64-labeled anti-colorectal carcinoma monoclonal antibody fragments 1A3-F(ab′)$_2$. J Nucl Med. 1995;36:850–858. [PubMed: 7738663]

28. Fujibayashi Y, Cutler CS, Anderson CJ, et al. Comparative studies of Cu-64-ATSM and C-11-acetate in an acute myocardial infarction model: ex vivo imaging of hypoxia in rats. Nucl Med Biol. 1999;26:117–121. [PubMed: 10096511]
29. Anderson CJ, Dehdashti F, Cutler PD, et al. $^{64}$Cu-TETA-octreotide as a PET imaging agent for patients with neuroendocrine tumors. J Nucl Med. 2001;42: 213–221. [PubMed: 11216519]
30. Gariepy J, Remy S, Zhang X, et al. A simple two-step approach for introducing a protected diaminedithiol chelator during solid-phase assembly of peptides. Bioconjug Chem. 2002;13:679–684. [PubMed: 12009962]
31. Gespach C, Bawab W, de Cremoux P, Calvo F. Pharmacology, molecular identification, and functional characteristics of VIP receptors in human breast cancer cells. Cancer Res. 1988;48:5079–5083. [PubMed: 2842044]
32. Surti S, Karp JS, Freifelder R, Perkins AE, Muehllenher G. Design evaluation of A-PET: a high sensitivity animal PET camera. IEEE Trans Nucl Sci. 2003;50: 1357–1363.
33. Daube-Witherspoon ME, Matej S, Karp JS, Lewitt RM. Application of the row action maximum likelihood algorithm with spherical basis functions to clinical PET imaging. IEEE Trans Nucl Sci. 2001;48:24–30.
34. Pena MMO, Lee J, Thiele DJ. A delicate balance: homeostatic control of copper uptake and distribution. J Nutr. 1999;129:1251–1260. [PubMed: 10395584]
35. Riggio M, Lee J, Scudiero R, Parisi E, Thiele DJ, Filosa S. High affinity copper transport protein in the lizard *Podarcis sicula*: molecular cloning, functional characterization, and expression in somatic tissues, follicular oocytes, and eggs. Biochim Biophys Acta. 2002;1576:127–135. [PubMed: 12031492]
36. Lewis MR, Wang M, Axworthy DB, et al. In vivo evaluation of pretargeted $^{64}$Cu for tumor imaging and therapy. J Nucl Med. 2003;44:1284–1292. [PubMed: 12902420]
37. Tatsumi M, Nakamoto Y, Traughber B, Marshall LT, Geschwind JFH, Wahl RL. Initial experience in small animal tumor imaging with a clinical positron emission tomography/computed tomography scanner using 2-[F-18]fluoro-2-deoxy-D-glucose. Cancer Res. 2003;63:6253–6357.
38. Wickstrom E, Tian X, Rao PS, Thakur ML, Qin W, Sauter ER. Oncogene mRNA imaging with $^{99m}$Tc-chelator-PNA-peptides. Russ Chem Bull. 2002;51:1083–1099.
39. Rao PS, Tian X, Qin W, et al. $^{99m}$Tc-Peptide-peptide nucleic acid probes for imaging oncogene mRNAs in tumours. Nucl Med Commun. 2003;34:857–863.
40. Lister-James J, Moyer BR, Dean T. Small peptides radiolabeled with $^{99m}$Tc. Q J Nucl Med. 1996;40:221–233. [PubMed: 8961801]

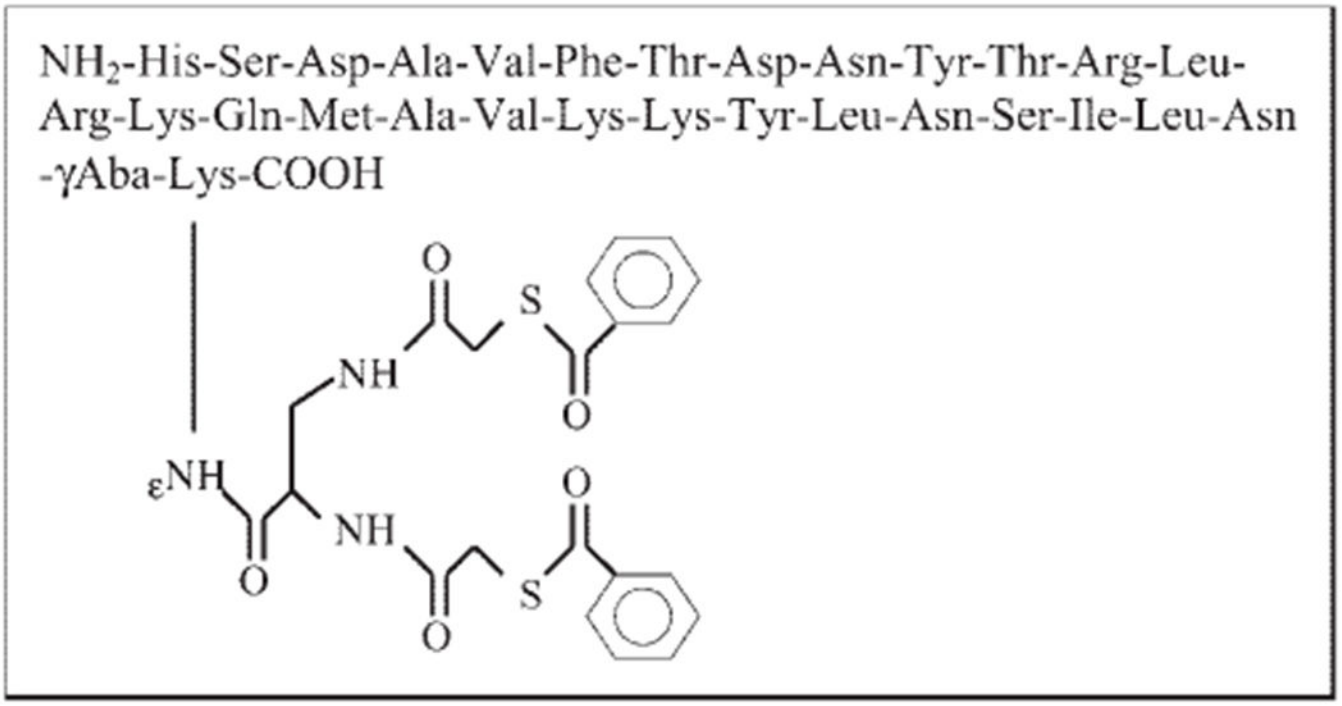


**FIGURE 1.**
Schematic presentation of TP3982.

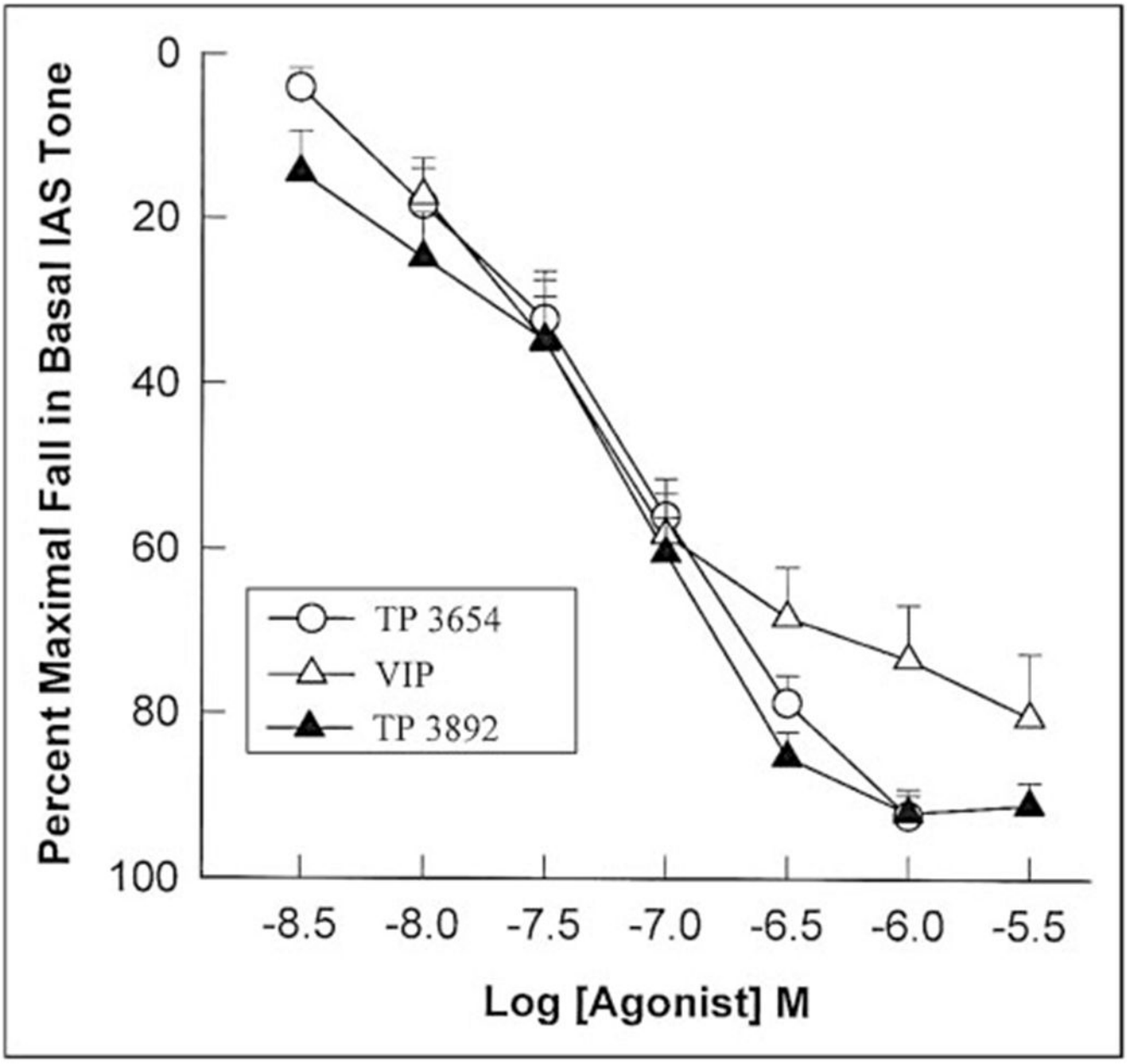


**FIGURE 2.**

Effect of increasing concentration of $VIP_{28}$, unlabeled TP3654, and unlabeled TP3982, on resting opossum IAS smooth muscle tissue. At $1 \times 10^{-6}$ mol/L TP3654 and TP3982, ~95% relaxivity was achieved with ~75% for $VIP_{28}$ at the same concentration. Data suggest that biologic activity of TP3982 was not compromised.

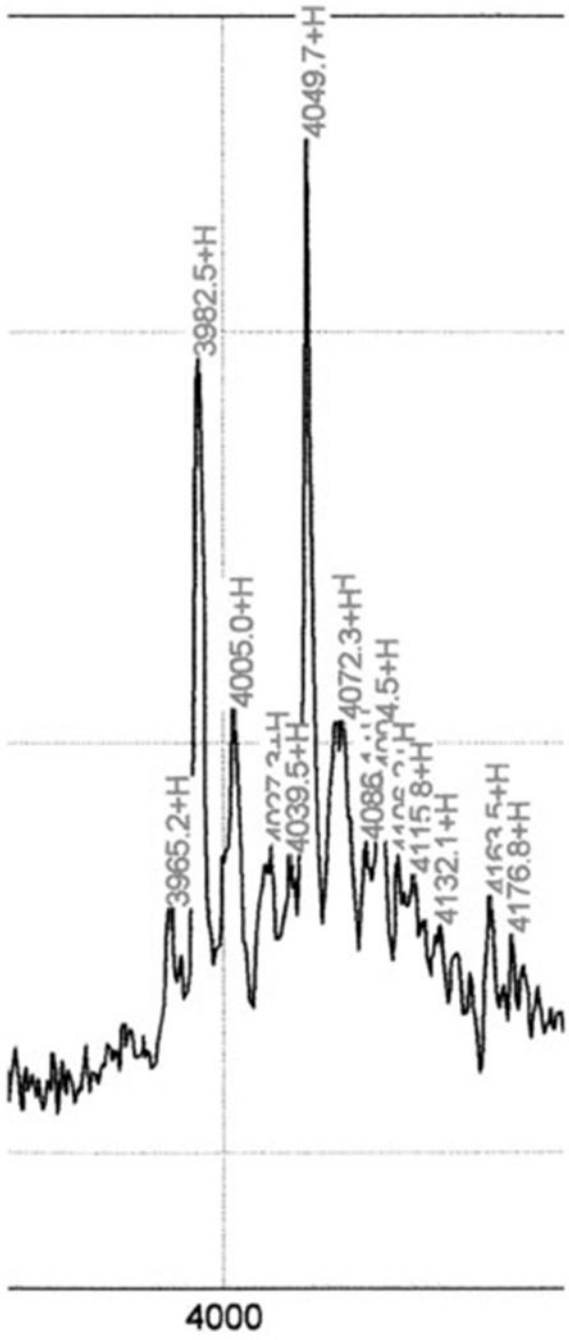


**FIGURE 3.**

SELDI-TOF-mass spectrum of Cu-TP3982 complex, depicting the complex mass of 4,049.7 Da and the mass of unreacted TP3982 at 3,982.7 Da.

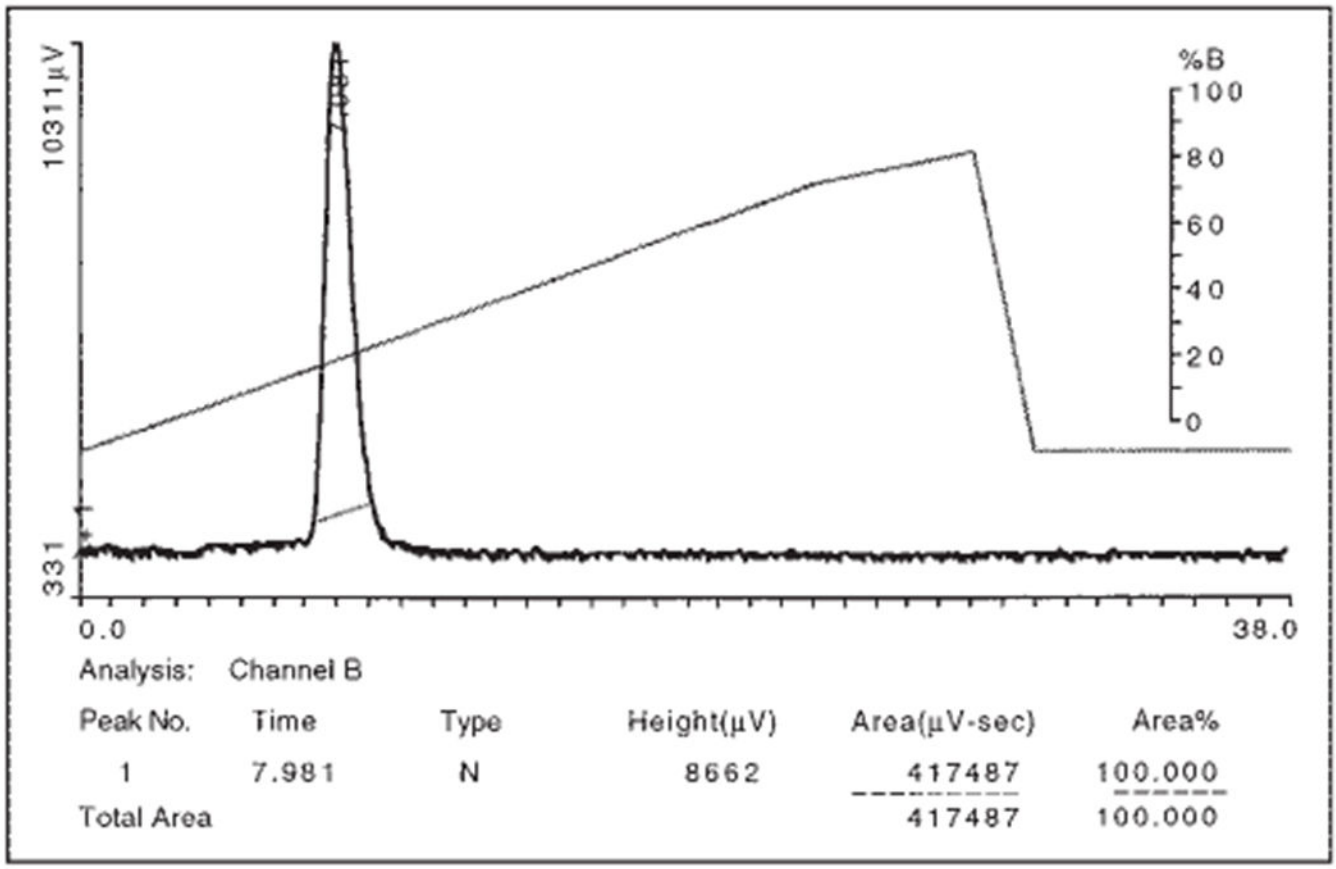


**FIGURE 4.**

HPLC elution profile of $^{64}$Cu-TP3982. 100% radioactivity was eluted in a single peak at $R_t$ 8 min. Unbound $^{64}$Cu elutes at $R_t$ 4.2 min. The diagonal line is percent solvent B (B = 0.1% TFA/ACN; A = 0.1% TFA/$H_2O$).

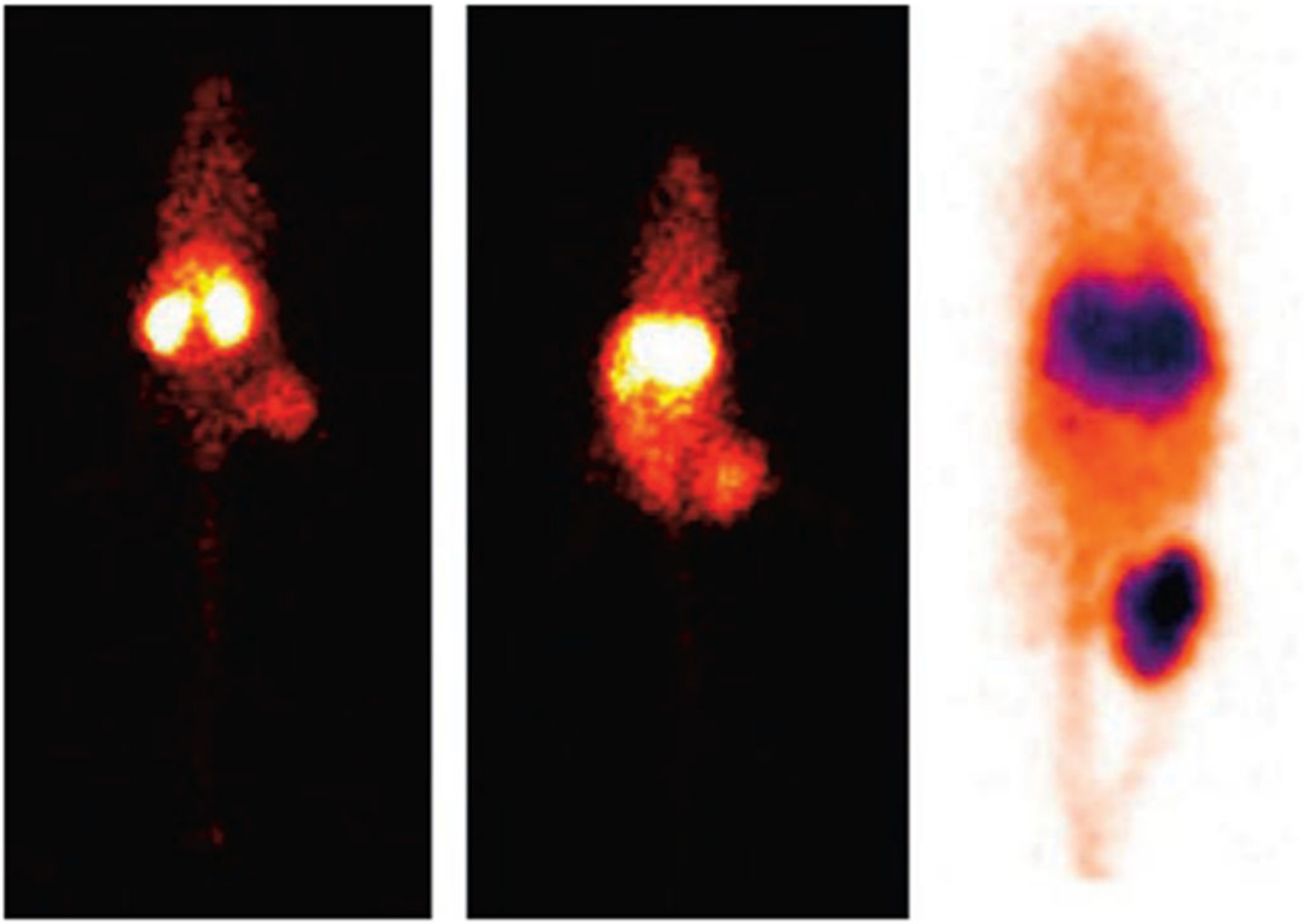

**FIGURE 5.**

Composite of 3 representative 24-h images of T47D human BC bearing nude mice receiving $^{99m}$Tc-TP3654 (left), $^{99m}$Tc-TP3982 (center), and $^{64}$Cu-TP3982 (right). The gray scale in the first 2 $\gamma$-camera images was 0 to 50. The 1-mm coronal PET image of a mouse given $^{64}$Cu-TP3982 shows enhanced uptake in the tumor. $\gamma$-Camera images are in posterior position. Tumor is in right flank in each mouse.

**TABLE 1**

Tissue Distribution (%ID/g) of $^{99m}$Tc-TP3654 and $^{99m}$Tc-TP3982 in Nude Mice Bearing T47D ($n$ = 5)

| | 4 h | | | 24 h | | |
|---|---|---|---|---|---|---|
| **Tissue** | **$^{99m}$Tc-TP3654** | **$^{99m}$Tc-TP3982** | ***P*** | **$^{99m}$Tc-TP3654** | **$^{99m}$Tc-TP3982** | ***P*** |
| Muscle | 0.09 ± 0.01 | 0.29 ± 0.07 | 0.01 | 0.04 ± 0.01 | 0.17 ± 0.04 | 0.00 |
| Intestine | 0.18 ± 0.05 | 0.64 ± 0.15 | 0.01 | 0.05 ± 0.01 | 0.28 ± 0.03 | 0.00 |
| Heart | 0.10 ± 0.00 | 1.25 ± 0.11 | 0.01 | 0.06 ± 0.01 | 0.47 ± 0.03 | 0.00 |
| Lungs | 0.17 ± 0.01 | 0.90 ± 0.11 | 0.01 | 0.16 ± 0.09 | 0.54 ± 0.05 | 0.00 |
| Blood | 0.21 ± 0.02 | 0.82 ± 0.08 | 0.01 | 0.12 ± 0.02 | 0.23 ± 0.01 | 0.00 |
| Spleen | 0.19 ± 0.05 | 1.98 ± 0.38 | 0.01 | 0.11 ± 0.02 | 1.29 ± 0.08 | 0.00 |
| Kidneys | 18.99 ± 3.75 | 7.70 ± 1.26 | 0.01 | 3.52 ± 0.40 | 5.18 ± 0.45 | 0.01 |
| Liver | 1.12 ± 0.08 | 10.13 ± 1.69 | 0.01 | 0.33 ± 0.04 | 6.11 ± 0.50 | 0.00 |
| Tumor | 0.24 ± 0.08 | 0.51 ± 0.05 | 0.01 | 0.23 ± 0.13 | 0.77 ± 0.12 | 0.00 |
| T/M ratio | 2.73 ± 1.09 | 1.86 ± 0.59 | 0.01 | 6.28 ± 3.09 | 4.83 ± 1.31 | 0.05 |
| T/B ratio | 1.16 ± 0.29 | 0.63 ± 0.12 | 0.01 | 1.98 ± 1.44 | 3.29 ± 0.55 | 0.04 |

T/M ratio = tumor-to-muscle ratio; T/B ratio = tumor-to-blood ratio.

**TABLE 2**

Tissue Distribution (%ID/g) of $^{64}$Cu-TP3982 and $^{99m}$Tc-TP3982 in Nude Mice Bearing T47D ($n$ = 5)

| | 4 h | | | 24 h | | |
|---|---|---|---|---|---|---|
| **Tissue** | **$^{64}$Cu-TP3982** | **$^{99m}$Tc-TP3982** | ***P*** | **$^{64}$Cu-TP3982** | **$^{99m}$Tc-TP3982** | ***P*** |
| Muscle | 1.77 ± 0.33 | 0.29 ± 0.07 | 0.01 | 2.68 ± 0.30 | 0.17 ± 0.04 | 0.00 |
| Intestine | 8.31 ± 2.83 | 0.64 ± 0.15 | 0.01 | 8.97 ± 3.03 | 0.28 ± 0.03 | 0.00 |
| Heart | 3.90 ± 1.07 | 1.25 ± 0.11 | 0.01 | 6.41 ± 1.92 | 0.47 ± 0.03 | 0.00 |
| Lungs | 50.40 ± 8.06 | 0.90 ± 0.11 | 0.01 | 11.02 ± 5.13 | 0.54 ± 0.05 | 0.00 |
| Blood | 2.27 ± 0.80 | 0.82 ± 0.08 | 0.01 | 2.80 ± 0.97 | 0.23 ± 0.01 | 0.00 |
| Spleen | 4.12 ± 1.52 | 1.98 ± 0.38 | 0.01 | 4.74 ± 1.61 | 1.29 ± 0.08 | 0.00 |
| Kidneys | 9.08 ± 3.23 | 7.70 ± 1.26 | 0.01 | 10.56 ± 3.59 | 5.18 ± 0.45 | 0.01 |
| Liver | 25.69 ± 2.73 | 10.13 ± 1.69 | 0.01 | 21.15 ± 8.08 | 6.11 ± 0.50 | 0.00 |
| Tumor | 10.81 ± 2.12 | 0.51 ± 0.05 | 0.01 | 17.04 ± 0.73 | 0.77 ± 0.12 | 0.00 |
| T/M ratio | 6.42 ± 2.30 | 1.86 ± 0.59 | 0.01 | 6.43 ± 0.86 | 4.83 ± 1.31 | 0.05 |
| T/B ratio | 5.96 ± 4.32 | 0.63 ± 0.12 | 0.01 | 6.99 ± 3.40 | 3.29 ± 0.55 | 0.04 |

T/M ratio = tumor-to-muscle ratio; T/B ratio = tumor-to-blood ratio.

**TABLE 3**

Four-Hour and 24-Hour Tissue Distribution (%ID/g) of $^{64}$Cu-TP3982 Before and After Receptor Blocking in Mice Bearing T47D Tumors ($n$ = 4)

| | 4 h | | | 24 h | | |
|---|---|---|---|---|---|---|
| **Tissue** | **Before** | **After** | ***P*** | **Before** | **After** | ***P*** |
| Muscle | 1.77 ± 0.33 | 1.16 ± 0.19 | 0.01 | 2.68 ± 0.30 | 1.61 ± 0.39 | 0.00 |
| Intestine | 8.31 ± 2.83 | 5.20 ± 0.59 | 0.01 | 8.97 ± 3.03 | 6.19 ± 0.63 | 0.02 |
| Heart | 3.90 ± 1.07 | 2.89 ± 0.34 | 0.01 | 6.41 ± 1.92 | 4.37 ± 0.60 | 0.01 |
| Lungs | 50.40 ± 8.06 | 5.36 ± 0.33 | 0.01 | 11.02 ± 5.13 | 7.12 ± 0.69 | 0.08 |
| Blood | 2.27 ± 0.80 | 2.00 ± 0.15 | 0.01 | 2.80 ± 0.97 | 2.91 ± 0.29 | 0.75 |
| Spleen | 4.12 ± 1.52 | 14.93 ± 4.01 | 0.01 | 4.74 ± 1.61 | 4.55 ± 1.15 | 0.77 |
| Kidneys | 9.08 ± 3.23 | 5.78 ± 0.24 | 0.01 | 10.56 ± 3.59 | 8.38 ± 0.28 | 0.13 |
| Liver | 25.69 ± 2.73 | 30.26 ± 3.59 | 0.12 | 21.15 ± 8.08 | 20.64 ± 1.84 | 0.88 |
| Tumor | 10.81 ± 2.12 | 6.42 ± 1.14 | 0.02 | 17.04 ± 0.73 | 12.06 ± 2.87 | 0.01 |
| T/M ratio | 6.42 ± 2.30 | 5.73 ± 1.79 | 0.83 | 6.43 ± 0.86 | 7.92 ± 3.26 | 0.34 |
| T/B ratio | 5.96 ± 4.32 | 3.21 ± 0.50 | 0.19 | 6.99 ± 3.40 | 4.17 ± 1.00 | 0.03 |

T/M ratio = tumor-to-muscle ratio; T/B ratio = tumor-to-blood ratio.